First-principles approach to electrorotation assay

2002 J. Phys.: Condens. Matter 14 1213

(http://iopscience.iop.org/0953-8984/14/6/308)

INSTITUTE OF PHYSICS PUBLISHING JOURNAL OF PHYSICS: CONDENSED MATTER

J. Phys.: Condens. Matter **14** (2002) 1213–1221 PII: S0953-8984(02)26977-5

First-principles approach to electrorotation assay

J P Huang and K W Yu

Department of Physics, The Chinese University of Hong Kong, Shatin, NT, Hong Kong, People's Republic of China

Received 19 July 2001, in final form 14 December 2001
Published 1 February 2002
Online at stacks.iop.org/JPhysCM/14/1213

Abstract

We have presented a theoretical study of electrorotation assay based on the spectral representation theory. We consider unshelled and shelled spheroidal particles as an extension to spherical ones. From the theoretical analysis, we find that the coating can change the characteristic frequency at which the maximum rotational angular velocity occurs. The shift in the characteristic frequency is attributed to a change in the dielectric properties of the bead–coating complex with respect to those of the uncoated particles. By adjusting the dielectric properties and the thickness of the coating, it is possible to obtain good agreement between our theoretical predictions and the assay data.

1. Introduction

When a suspension of colloidal particles or biological cells is exposed to an external electric field, the analysis of the frequency-dependent response yields valuable information on various processes, like the structural (Maxwell–Wagner) polarization effects [1, 2]. The polarization is characterized by a variety of characteristic frequency-dependent changes. While the polarization of biological cells can be investigated by the method of dielectric spectroscopy [3], conventional dielectrophoresis and electrorotation (ER) analyse the frequency dependence of translations and rotations of single cells in an inhomogeneous and rotating external field, respectively [4, 5]. With the recent advent of experimental techniques such as automated video analysis [6] as well as light scattering methods [2], the cell movements can be accurately monitored. In ER, the frequency dependence of the polarization leads to a phase shift between the induced dipole moment and the rotating field, giving rise to a torque acting on the particle which causes the rotation of the individual particle.

The phenomenon of ER can be developed into a useful technique known as ER assay. The ER assay combines antibody technology with ER to detect analytes in aqueous solutions. The analyte to be detected is bound to a latex bead of known dielectric properties to form the analyte-bead complex, which causes a change in the dielectric properties. The change can be detected by ER technique, thus allowing the rapid and accurate detection of analytes in aqueous solutions. This method can be used to detect various analytes, the selection of which can be controlled by the proper choice of binding agents.

0953-8984/02/061213+09$30.00

In this work, we propose the use of the spectral representation [7] for analysing the ER of particles in suspensions. The spectral representation is a rigorous mathematical formalism for the effective dielectric constant of a two-phase composite material [7]. It offers the advantage of the separation of materials parameters (namely the dielectric constant and conductivity) from the cell structure information, thus simplifying the study. From the spectral representation, one can readily derive the dielectric dispersion spectrum, with the dispersion strength as well as the characteristic frequency being explicitly expressed in terms of the structure parameters and the materials parameters of the cell suspension (see section 2.2 below). The actual shape of the real and imaginary parts of the permittivity over the relaxation region can be uniquely determined by the Debye relaxation spectrum, parametrized by the characteristic frequencies and the dispersion strengths. So, we can study the impact of these parameters on the dispersion spectrum directly. The same formalism has been used recently to study the dielectric behaviour of cell suspensions [8].

In this connection, we mention alternative methods—namely, solving Laplace's equation directly and Gimsa's approach based on equivalent circuits [1, 2]. To our knowledge, none of these methods separates microstructure parameters from materials information.

2. Formalism

We regard a suspension as a composite system consisting of spherical or spheroidal particles of complex dielectric constant $\tilde{\epsilon}_1$ dispersed in a host medium of $\tilde{\epsilon}_2$. A uniform electric field $\boldsymbol{E}_0 = E_0\hat{\boldsymbol{z}}$ is applied to the composites along the z-axis. We briefly review the spectral representation theory of the effective dielectric constant to establish notation.

2.1. Spectral representation

The spectral representation is a mathematical transformation of the complex effective dielectric constant $\tilde{\epsilon}_e$. In its original form [7], a two-phase composite material is considered, in which inclusions of complex dielectric constant $\tilde{\epsilon}_1$ and volume fraction p are randomly embedded in a host medium of dielectric constant $\tilde{\epsilon}_2$. The complex effective dielectric constant $\tilde{\epsilon}_e$ will in general depend on the constituent dielectric constants, and the volume fraction of inclusions, as well as the detailed microstructure of the composite materials.

The essence of the spectral representation is defining the following transformations. If we denote a complex material parameter

$$\tilde{s} = \left(1 - \frac{\tilde{\epsilon}_1}{\tilde{\epsilon}_2}\right)^{-1} \tag{1}$$

then the reduced effective dielectric constant

$$w(\tilde{s}) = 1 - \frac{\tilde{\epsilon}_e}{\tilde{\epsilon}_2} \tag{2}$$

can be written as

$$w(\tilde{s}) = \sum_n \frac{F_n}{\tilde{s} - s_n} \tag{3}$$

where n is a positive integer, i.e., $n = 1, 2, \ldots$, and F_n and s_n are the nth microstructure parameters of the composite materials [7]. In equation (3), $0 \leqslant s_n < 1$ is a real number, while F_n satisfies a sum rule [7]:

$$\sum_n F_n = p \tag{4}$$

where p is the volume fraction of the suspended cells.

As a result, the spectral representation is a useful theory which helps separate the materials properties from the geometric information. In what follows, we illustrate the spectral representation using a capacitance with simple geometry. In particular, a parallel-plate capacitor is considered as an example. We will discuss two cases, namely, the series combination and the parallel combination.

In the first case, if one inserts a dielectric slab of dielectric constant $\tilde{\epsilon}_1$ and thickness h_1, as well as a dielectric of dielectric constant $\tilde{\epsilon}_2$ and thickness h_2 (of the same area A) into a parallel-plate capacitor of total thickness $h = h_1 + h_2$, the overall capacitance C is given by

$$C^{-1} = C_1^{-1} + C_2^{-1}$$

where $C_1 = \tilde{\epsilon}_1 A/h_1$ and $C_2 = \tilde{\epsilon}_2 A/h_2$, A being the area of a plate. On the other hand, we may define the equivalent capacitance as $C = \tilde{\epsilon}_e A/h$, where $\tilde{\epsilon}_e$ is the effective dielectric constant. That is, we replace the composite dielectric by a homogeneous dielectric of dielectric constant $\tilde{\epsilon}_e$.

Let $\tilde{\epsilon}_1 = \tilde{\epsilon}_2(1 - 1/\tilde{s})$; we can express C in the spectral representation:

$$C = \frac{A\tilde{\epsilon}_2}{h} - \frac{A\tilde{\epsilon}_2 h_1/h^2}{\tilde{s} - h_2/h}.$$

In accord with the spectral representation, one may introduce $w(\tilde{s}) = 1 - \tilde{\epsilon}_e/\tilde{\epsilon}_2$, which is in fact the same as $w(\tilde{s}) = 1 - C/C_0$, where C_0 is the capacitance when the plates are all filled with a dielectric material of dielectric constant $\tilde{\epsilon}_2$—that is, $C_0 = \tilde{\epsilon}_2 A/h$. Thus we obtain

$$w(\tilde{s}) = \frac{h_1/h}{s - h_2/h}$$

from which we find that the material parameter is separated from the geometric parameter. Comparison of $w(\tilde{s})$ with equation (3) yields

$$F_1 = h_1/h \qquad s_1 = h_2/h.$$

We should remark that F_1 obtained herein is just equal to the volume fraction of the dielectric of dielectric constant $\tilde{\epsilon}_1$, and that s_1 satisfies $0 \leqslant s_1 < 1$, as required by the spectral representation theory.

Next we consider the parallel combination. If one inserts a material of dielectric constant $\tilde{\epsilon}_1$ and area w_1 as well as a dielectric of dielectric constant $\tilde{\epsilon}_2$ and area w_2 (of the same thickness h) into a parallel-plate capacitor of total area $A = w_1 + w_2$, the overall capacitance C is given by

$$C = C_1 + C_2$$

where $C_1 = \tilde{\epsilon}_1 w_1/h$ and $\tilde{\epsilon}_2 = \tilde{\epsilon}_2 w_2/h$. Similarly, after introducing the effective dielectric constant $\tilde{\epsilon}_e$, we may define the overall capacitance as $C = \tilde{\epsilon}_e A/h$.

Again, in the spectral representation, let $\tilde{\epsilon}_1 = \tilde{\epsilon}_2(1 - 1/\tilde{s})$; then

$$C = \frac{\tilde{\epsilon}_2 A}{h} - \frac{\tilde{\epsilon}_2 w_1}{h\tilde{s}}.$$

Writing $w(\tilde{s}) = 1 - C/C_0$, we obtain

$$w(\tilde{s}) = \frac{w_1/A}{\tilde{s}}.$$

From this equation, the material parameter is also found to be separated from the geometric parameter. It is clear that $F_1 = w_1/A$, i.e., the volume fraction of the dielectric of dielectric constant $\tilde{\epsilon}_1$, and $s_1 = 0$.

2.2. Shelled spheroidal particle model

For inclusions of arbitrary shape, the spectral representation can only be solved numerically [7]. However, analytic solutions can be obtained for isolated spherical and ellipsoidal particles. For dilute suspensions of prolate spheroidal particles, the particles can be regarded as noninteracting. The problem is simplified to the calculation of s_n with a single particle, which can be solved exactly.

In fact, the suspension of shelled spheroidal particles dispersed in a host medium is a three-component system. Although the spectral representation is generally valid for two-component composites, we have recently shown that it also applies to composites of coated spheres randomly embedded in a host medium [9]. Similarly, we will show that the spectral representation also applies to the suspension of spheroidal particles of complex dielectric constant $\tilde{\epsilon}_1$ coated with a shell of dielectric constant $\tilde{\epsilon}_s$ dispersed in a host medium of $\tilde{\epsilon}_2$, where

$$\tilde{\epsilon} = \epsilon + \sigma/\mathrm{i}\,2\pi f \tag{5}$$

where f is the frequency of the applied field. In what follows, we will show that from the spectral representation, one can obtain the analytic expressions for the characteristic frequency at which the maximum ER velocity occurs. The depolarization factors of the spheroidal particles will be described by a sum rule

$$L_z + 2L_{xy} = 1 \tag{6}$$

where $0 < L_z \leqslant 1/3$ and L_{xy} are the depolarization factors along the z- and x- (or y-) axes of the spheroidal particle, respectively. In fact, $L_z = L_{xy} = 1/3$ just indicates a spherical particle.

The phenomenon of ER is based on the interaction between a time-varying electric field $\boldsymbol{E}$ and the induced dipole moment $\boldsymbol{M}$. The dipole moment of the particle arises from the induced charges that accumulate at the interface of the particle. As the prolate spheroidal particles are easily oriented along their long axes by the rotating field, we consider the orientation in which the long axis lies within the field plane [10][1]. In fact, the extension of our theory to deal with oblate spheroid is straightforward. In doing so, it suffices to consider $1/3 < L_z < 1$ and the formalism will remain unchanged.

The angle between $\boldsymbol{M}$ and $\boldsymbol{E}$ is denoted by θ, where $\theta = \omega \times$ time and $\omega = 2\pi f$ is the angular velocity of the rotating electric field. The torque acting on the particle is given by the vector cross product between the electric field and the dipole moment, so only the imaginary part of the dipole moment contributes to the ER response. In the steady state, the frequency-dependent rotation speed $\Omega(f)$, which results from the balance between the torque and the viscous drag, is given by

$$\Omega(f) = -F(\epsilon_2, E, \eta)\,\mathrm{Im}(\tilde{b}_z\langle\cos^2\theta\rangle + \tilde{b}_{xy}\langle\sin^2\theta\rangle) = -F(\epsilon_2, E, \eta)\,\mathrm{Im}(\tilde{b}_z/2 + \tilde{b}_{xy}/2) \tag{7}$$

where E is the strength of the applied electric field and F is a coefficient which is inversely proportional to the dynamic viscosity η of the host medium. For spherical cells, $F = -\epsilon_2 E^2/2\eta$. In equation (7), $\mathrm{Im}(\cdots)$ indicates the imaginary parts of $(\cdots)$, and the angular brackets denote a time average. Since the angular velocity of the rotating field is much greater than the ER angular velocity, i.e., $\omega \gg \Omega$, the time averages are just equal to $1/2$. For a single coated spheroidal particle, the dipole factor $\tilde{b}_z$ is given by [11]

$$\tilde{b}_z = \frac{1}{3}\frac{(\tilde{\epsilon}_s - \tilde{\epsilon}_2)[\tilde{\epsilon}_s + L_z(\tilde{\epsilon}_1 - \tilde{\epsilon}_s)] + (\tilde{\epsilon}_1 - \tilde{\epsilon}_s)y[\tilde{\epsilon}_s + L_z(\tilde{\epsilon}_2 - \tilde{\epsilon}_s)]}{(\tilde{\epsilon}_s - \tilde{\epsilon}_1)(\tilde{\epsilon}_2 - \tilde{\epsilon}_s)yL_z(1 - L_z) + [\tilde{\epsilon}_s + (\tilde{\epsilon}_1 - \tilde{\epsilon}_s)L_z][\tilde{\epsilon}_2 + (\tilde{\epsilon}_s - \tilde{\epsilon}_2)L_z]} \tag{8}$$

[1] It is not always necessary that prolate particles orient with their longest axis in the field plane. Depending on frequency, object and medium properties, a perpendicular orientation can be observed, see e.g., [10].

where y is the volume ratio of the core to the whole coated spheroid, while b_{xy} can be obtained by replacing L_z with L_{xy} in equation (8).

We are now in a position to represent b_z and b_{xy} in the spectral representation. Let $\tilde{\epsilon}_1 = \tilde{\epsilon}_2(1 - 1/\tilde{s})$, and assume $x = \tilde{\epsilon}_s/\tilde{\epsilon}_2$; we obtain

$$\tilde{b}_z = \mathrm{NP} + \frac{F_1}{\tilde{s} - s_1} \tag{9}$$

where NP denotes the nonresonant part [9] which vanishes in the limit of unshelled spheroidal cells. In equation (9), the various quantities are given by

$$s_1 = -\frac{\beta}{\gamma} \tag{10}$$

$$F_1 = \frac{-x^2 y}{\alpha\gamma} \tag{11}$$

$$\mathrm{NP} = \frac{-L_z + L_z y + x(-1 + 2L_z + y - 2L_z y) + x^2(1 - L_z - y + L_z y)}{\alpha} \tag{12}$$

where

$$\alpha = 3L_z - 3L_z^2 - 3L_z y + 3L_z^2 y + x(3 - 6L_z + 6L_z^2 + 6L_z y - 6L_z^2 y) \times x^2(3L_z - 3L_z^2 - 3L_z y + 3L_z^2 y)$$

$$\beta = -L_z + L_z^2 + L_z y - L_z^2 y + x(-L_z^2 - L_z y + L_z^2 y)$$

$$\gamma = L_z - L_z^2 - L_z y + L_z^2 y + x(1 - 2L_z + 2L_z^2 + 2L_z y - 2L_z^2 y) + x^2(L_z - L_z^2 - L_z y + L_z^2 y).$$

Note that we have assumed x to be a real number, which will be justified below. After substituting $\tilde{\epsilon} = \epsilon + \sigma/\mathrm{i}2\pi f$ into equation (9), we rewrite $\tilde{b}_z$ after simple manipulations as

$$\tilde{b}_z = \left(\mathrm{NP} + \frac{F_1}{s - s_1}\right) + \frac{\delta\epsilon_1}{1 + \mathrm{i}f/f_{c1}} \tag{13}$$

with $s = (1 - \epsilon_1/\epsilon_2)^{-1}$ and $t = (1 - \sigma_1/\sigma_2)^{-1}$, where

$$\delta\epsilon_1 = F_1 \frac{s - t}{(t - s_1)(s - s_1)}$$

$$f_{c1} = \frac{1}{2\pi}\frac{\sigma_2}{\epsilon_2}\frac{s(t - s_1)}{t(s - s_1)}.$$

Similarly, we may rewrite $\tilde{b}_{xy}$ as

$$\tilde{b}_{xy} = \left(\mathrm{NP}' + \frac{F_2}{s - s_2}\right) + \frac{\delta\epsilon_2}{1 + \mathrm{i}f/f_{c2}}. \tag{14}$$

Therefore, we obtain

$$\delta\epsilon_2 = F_2 \frac{s - t}{(t - s_2)(s - s_2)}$$

$$f_{c2} = \frac{1}{2\pi}\frac{\sigma_2}{\epsilon_2}\frac{s(t - s_2)}{t(s - s_2)}.$$

Note that NP′, s_2, and F_2 are obtained by replacing L_z with L_{xy} in the expressions for NP, s_1, and F_1, respectively.

We have thus predicted that two characteristic frequencies may appear for uncoated or coated spheroidal particles. Previous theories were often limited to spherical particles, i.e., $L_z = L_{xy} = 1/3$. Therefore, only one characteristic frequency exists. We should remark that even though two characteristic frequencies are predicted, only one of them is dominant (see below).

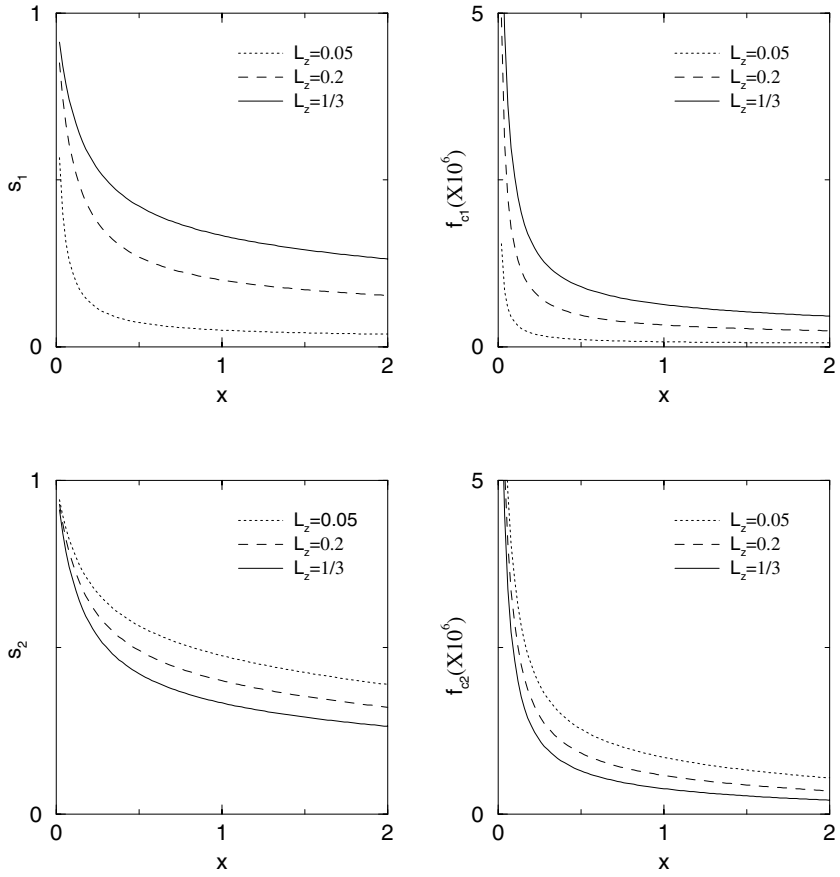

Figure 1. Upper panels: s_1 and f_{c1} plotted against x for different L_z at $z = 2$. Lower panels: s_2 and f_{c2} plotted against x for different L_z at $z = 2$.

3. Numerical calculations

The model put forward in the previous section applies to various systems such as biological cells and polystyrene beads. Here we perform numerical calculations to investigate the characteristic frequency. Let $s = 1.1$, $t = -0.005$, and $\epsilon_2 = 80\epsilon_0$, where ϵ_0 is the dielectric constant of the vacuum. In figure 1, we investigate the effect of particle shape on s_1 and f_{c1} (upper panels), and s_2 and f_{c2} (lower panels), for $z = 2$ and $\sigma_2 = 2.9 \times 10^{-5}$ S m^{-1}, where $z = 1/y$, and $z^{1/3} > 1$ reflects the thickness of the shell (or coating). As is evident from the figure, an increase in the dielectric constant ratio x leads to a red-shift of the characteristic frequency. For a certain x, a small depolarization factor—i.e., the particle deviates substantially from spherical shape, may yield a red-shift too.

In figure 2, we investigate the effect of the depolarization factor on the quantities $-\mathrm{Im}[b_z]/2$ and $-\mathrm{Im}[b_z/2 + b_{xy}/2]$. It is evident that the effect of b_{xy} on the peak is small when L_z is small, whereas it is large when L_z is large. Generally speaking, the dipole moment along the x- (or y-) axis strongly affects both the location and the magnitude of the peak of the rotation speed. For spheroidal particles, only one peak is found, and the other peak predicted by the theory may be too small to observe.

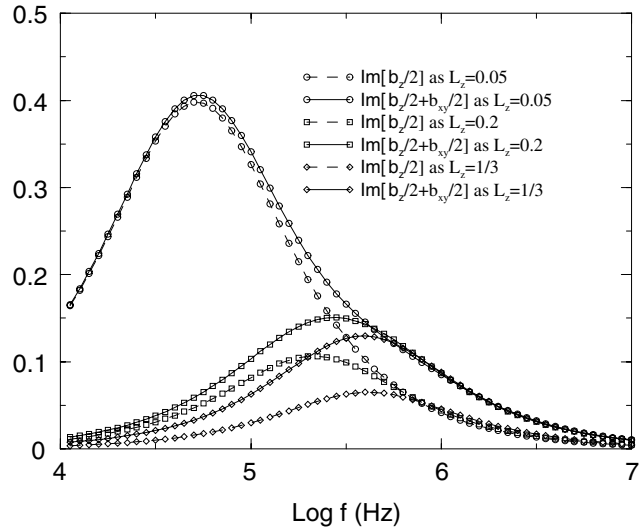

Figure 2. $-\mathrm{Im}(b_z/2 + b_{xy}/2)$ and $-\mathrm{Im}b_z/2$ are plotted against frequency ω for different L_z at $z = 6$, $x = 2$, and $\sigma_2 = 2.9 \times 10^{-5}$ S m^{-1}.

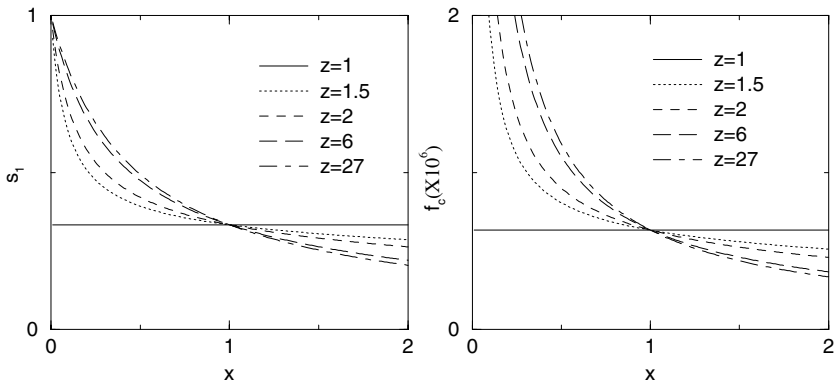

Figure 3. s_1 and f_c are plotted versus x for different z as $L_z = 1/3$ (i.e., spherical shape).

In order to validate our theory, here we considered the spherical particles as a limiting case of our model. In figure 3, s_1 and f_c are plotted versus x for a spherical bead ($L_z = 1/3$), for different z at $\sigma_2 = 2.9 \times 10^{-5}$ S m^{-1}. For large x, the shell thickness has only a minor effect on the characteristic frequency. Moreover, a thick shell leads to a red-shift (blue-shift) of the characteristic frequency appearing when $x > 1$ ($x < 1$). Also, all the f_c predicted for the different z are smaller (larger) than that predicted at $z = 1$ (i.e., for the uncoated bead) for $x > 1$ ($x < 1$).

At $x = 1$, i.e., when the shell has the same dielectric constant as the host, all the characteristic frequencies predicted for different thicknesses of shell are the same. Similar conclusions can be obtained not only for spherical shape, but also for prolate spheroidal shape (not shown here).

We attempt to fit our theoretical predictions with experimental data, which are extracted from an assay [12][2]. In this assay, three cases were studied, all dealing with spherical

[2] See also http://www.ibmm.informatics.bangor.ac.uk/pages/science/rot.htm for the basic science of ER.

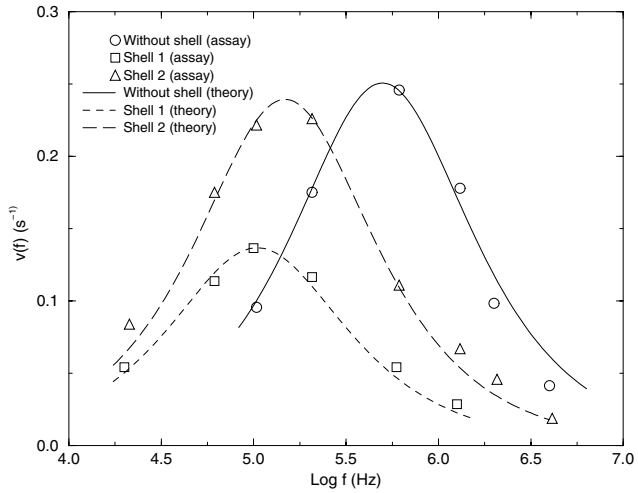

Figure 4. Curve fitting for $L_z = 1/3$ (i.e., spherical particles).

particles—that is, uncoated beads, beads coated with an antibody with specificity for Giardia (shell 1), and beads coated with an antibody with specificity for Cryptosporidium (shell 2). The bead diameter is 6 μm according to Burt *et al* [12], while Giardia and Cryptosporidium are both 0.8 μm in diameter. Let $\sigma_2 = 2.18 \times 10^{-5}$ S m^{-1}, $z = 6$, $x = 7.06$ (shell 1) and 4.63 (shell 2), and $F = 0.353$ (without shell), 1.629 (shell 1), and 2.278 (shell 2). Good agreement between our theoretical predictions and the assay data is shown in figure 4. From our theory, it is easy to find the corresponding characteristic frequencies at which maximum rotational angular velocity occurs, $f_c = 4.755 \times 10^5$ Hz (without shell), 10^5 Hz (shell 1), and 1.415×10^5 Hz (shell 2). From this, we find that the coating leads to a red-shift of the characteristic frequency. This is because the dielectric properties of the bead–coating complex have been changed.

We used $x > 1$ in our fitting, i.e., $x = 7.06$ and 4.63 for beads coated with an antibody with specificity for Giardia and Cryptosporidium, respectively. It is known that biological cells, such as Giardia and Cryptosporidium, have structures such as the cell wall, the plasma membrane, and the cytoplasm, where the cell wall has a larger conductivity than the suspending medium. Hence, we may safely take $x > 1$.

4. Discussion and conclusions

Here we would like to add some comments. We would like to clarify the assumptions in our model in more detail. In fact, there is only one peak (rather than two) for each polarization in our theory. This is because we assumed the ratio of the shell to the host dielectric constant x to be a real and positive number. If we had retained the (small) imaginary part of x in our calculation, then we would have had two peaks for each polarization. The conductivity-dominated peak would have occurred at substantially lower frequency. Thus, the effect of the neglect of the imaginary part of x is to drop the lower-frequency peak. Moreover, according to our calculations, there is one dominant pole associated with b_z and two (degenerate) sub-dominant poles associated with b_{xy} in the spectral representation. Thus, for shelled particles in the present work, only one peak has been shown.

We developed simple equations to describe the ER of particles in a suspension from the spectral representation. These equations serve as a basis for describing the parameter

dependence of the polarization and thereby enhance the applicability of various cell models in the analysis of polarization mechanisms. In this connection, the shelled spheroidal particle cell model may readily be extended to a multi-shell cell model. However, we believe that the multi-shell nature of a cell may have only a minor effect on the ER spectrum.

We have considered the case of an isolated cell, which is a valid assumption for low concentration of cells. However, for a higher concentration of cells, we should consider the mutual interaction between cells. For a randomly dispersed cell suspension, we may replace the dielectric constant of the host medium by the effective dielectric constant of the whole suspension.

When a strong rotating electric field is applied to a suspension, the induced dipole moment will induce an overall attractive force between the polarized cells, leading to rapid formation of sheet-like structures in the plane of the rotating field. In reality there is a phase shift between the induced dipole moment of the structure and the applied field, and this can lead to ER. However, the situation will be much more difficult than the single-cell case that we have studied because the many-body as well as multipolar interactions between the particles will produce a complicated ER spectrum. Fortunately, our recently developed integral equation formalism [13] can definitely help in solving for the Maxwell–Wagner relaxation spectrum.

In summary, we have presented a theoretical study of ER assay based on the spectral representation theory. We consider unshelled and shelled spheroidal particles as an extension to spherical ones. From the theoretical analysis, we find that the coating can change the characteristic frequency at which the maximum rotational angular velocity occurs. By adjusting the dielectric properties and the thickness of the coating, it was possible to obtain good agreement between our theoretical predictions and the assay data.

Note added in proof. We have recently reported the electrorotation of two spherical particles [14].

Acknowledgments

This work was supported by the Research Grants Council of the Hong Kong SAR Government under grant CUHK 4245/01P. JPH is grateful to Dr L Gao and Dr C Xu for fruitful discussion. KWY acknowledges the hospitality of Professor Hong Sun enjoyed during a visit to the University of California at Berkeley, and useful discussion with Professor G Q Gu.

References

[1] For a review, see Gimsa J and Wachner D 1999 *Biophys. J.* **77** 1316
[2] Gimsa J 1999 *Ann. NY Acad. Sci.* **873** 287
[3] Asami K, Hanai T and Koizumi N 1980 *Japan. J. Appl. Phys.* **19** 359
[4] Fuhr G, Gimsa J and Glaser R 1985 *Stud. Biophys.* **108** 149
[5] Gimsa J, Marszalek P, Lowe U and Tsong T Y 1991 *Biophys. J.* **73** 3309
[6] De Gasperis G, Wang X-B, Yang J, Becker F F and Gascoyne P R C 1998 *Meas. Sci. Technol.* **9** 518
[7] Bergman D J 1978 *Phys. Rep.* **43** 379
[8] Lei J, Jones T K Wan, Yu K W and Hong Sun 2001 *Phys. Rev.* E **64** 012903
[9] Yuen K P and Yu K W 1997 *J. Phys.: Condens. Matter* **9** 4669
[10] Gimsa J 2001 *Bioelectrochemistry* **54** 23
[11] Gao L, Jones T K Wan, Yu K W and Li Z Y 2000 *J. Phys.: Condens. Matter* **12** 6825
[12] Burt J P H, Chan K L, Dawson D, Parton A and Pethig R 1996 *Ann. Biol. Clin.* **54** 253
[13] Yu K W, Hong Sun and Jones T K Wan 2000 *Physica* B **279** 78
[14] Huang J P, Yu K W and Gu G Q 2002 *Phys. Rev.* E **65** 021401